Article

DNA as Helical Ruler: Exciton-Coupled Circular Dichroism in DNA Conjugates

Frederick D. Lewis, Ligang Zhang, Xiaoyang Liu, Xiaobing Zuo, David M. Tiede, Hai Long, and George C. Schatz

J. Am. Chem. Soc., **2005**, 127 (41), 14445-14453• DOI: 10.1021/ja0539387 • Publication Date (Web): 21 September 2005

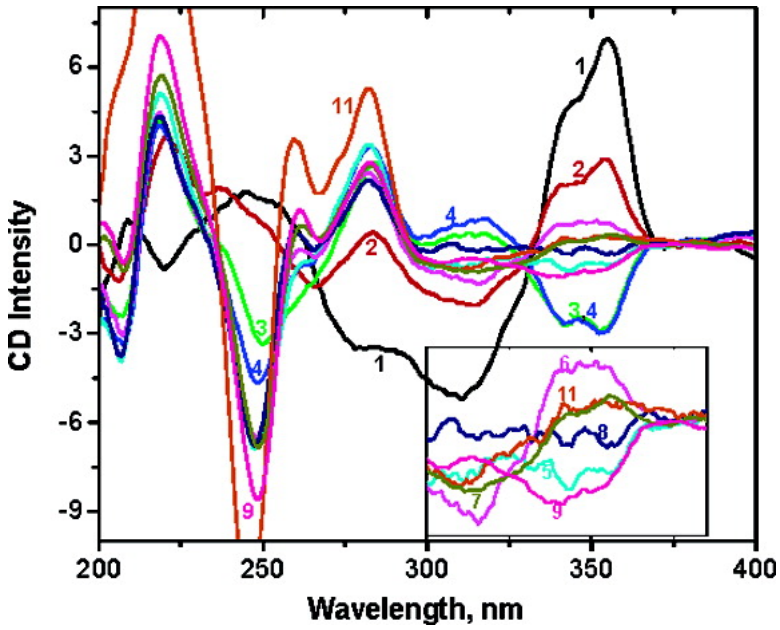

More About This Article

Additional resources and features associated with this article are available within the HTML version:

- Supporting Information
- Links to the 14 articles that cite this article, as of the time of this article download
- Access to high resolution figures
- Links to articles and content related to this article
- Copyright permission to reproduce figures and/or text from this article

View the Full Text HTML

J|A|C|S
ARTICLES
Published on Web 09/21/2005

DNA as Helical Ruler: Exciton-Coupled Circular Dichroism in DNA Conjugates

Frederick D. Lewis,*,† Ligang Zhang,† Xiaoyang Liu,† Xiaobing Zuo,‡ David M. Tiede,‡ Hai Long,† and George C. Schatz†

Contribution from the Department of Chemistry, Northwestern University, Evanston, Illinois 60208-3113, and Chemistry Division, Argonne National Laboratory, Argonne, Illinois 60439

Received June 14, 2005; E-mail: lewis@chem.northwestern.edu

Abstract: The structure and properties of oligonucleotide conjugates possessing stilbenedicarboxamide chromophores at both ends of a poly(dA):poly(dT) base-pair domain of variable length have been investigated using a combination of spectroscopic and computational methods. These conjugates form capped hairpin structures in which one stilbene serves as a hairpin linker and the other as a hydrophobic end-cap. The capping stilbene stabilizes the hairpin structures by ca. 2 kcal/mol, making possible the formation of a stable folded structure containing a single A:T base pair. Exciton coupling between the stilbene chromophores has little effect on the absorption bands of capped hairpins. However, exciton-coupled circular dichroism (EC-CD) can be observed for capped hairpins possessing as many as 11 base pairs. Both the sign and intensity of the EC-CD spectrum are sensitive to the number of base pairs separating the stilbene chromophores, as a consequence of the distance and angular dependence of exciton coupling. Calculated spectra obtained using a static vector model based on canonical B-DNA are in good agreement with the experimental spectra. Molecular dynamics simulations show that conformational fluctuations of the capped hairpins result in large deviations of the averaged spectra in both the positive and negative directions. These results demonstrate for the first time the ability of B-DNA to serve as a helical ruler for the study of electronic interactions between aligned chromophores. Furthermore, they provide important tests for atomistic theoretical models of DNA.

Introduction

The idealized linear helical structures of nucleic acid duplexes make them well suited for use as molecular rulers. The distance between two base pairs can be calculated from the average π-stacking distance, 3.4 Å per step in B-DNA, and the angle between any two base pairs can be calculated from the average vector angle between adjacent base pairs, 36°.[1] The control of distance within base-pair domains has been used extensively in studies of DNA electron transfer.[2] However, neither tunneling nor hopping mechanisms for long-range electron transfer of DNA are dependent on the helicity of DNA. The efficiency of fluorescence energy transfer between chromophores attached to complementary strands of DNA or RNA is dependent on the vector distance between chromophores and not simply the number of base pairs, and thus is dependent on the duplex helicity.[3] A graded set of RNA anticodon stem-loop probes possessing a 5-tethered iron has been used as a helical ruler to map the inside of the ribosome in messenger RNA.[4] Strand cleavage by iron-generated hydroxyl radicals occurs selectively at positions separated by 10 base pairs.

We recently reported the observation of exciton-coupled circular dichroism (EC-CD) between stilbene chromophores separated by 1−11 A:T base pairs in a collection of capped hairpin DNA conjugates (Chart 1, structures **1**−**6**, **8**, and **11**).[5] EC-CD has previously been used to investigate the structure and stereochemistry of both conformationally rigid and fluctional molecules;[6] however, it had not been used to investigate the helicity of biopolymers prior to our study. We observed that both the sign and intensity of the EC-CD spectra of the capped hairpins are dependent on the distance and dihedral angle between the two stilbenes, which are determined by the number of intervening base pairs. Good agreement between the experimental spectra and calculated spectra were obtained using a simple vector model and idealized B-DNA geometric parameters. Strong EC-CD has also been reported by Balaz et al. for two porphyrin chromophores attached to the 3′ and 5′ ends of complementary octanucleotides.[7]

† Northwestern University.
‡ Argonne National Laboratory.

(1) Neidle, S. *Oxford Handbook of Nucleic Acid Structure*; Oxford University Press: Oxford, 1999.
(2) Schuster, G. B., Ed. *Long-Range Charge Transfer in DNA*; Springer-Verlag: Berlin, 2004; Vol. 236−237.
(3) (a) Clegg, R. M. *Methods Enzymol.* **1992**, *211*, 353−388. (b) Clegg, R. M.; Murchie, A. I. H.; Zechel, A.; Lilley, D. M. J. *Proc. Natl. Acad. Sci. U.S.A.* **1993**, *90*, 2994−2998. (c) Hurley, D. J.; Tor, Y. *J. Am. Chem. Soc.* **2002**, *124*, 13231−13241.
(4) Joseph, S.; Weiser, B.; Noller, H. F. *Science* **1997**, *278*, 1093−1098.
(5) Lewis, F. D.; Liu, X.; Wu, Y.; Zuo, X. *J. Am. Chem. Soc.* **2003**, *125*, 12729−12731.
(6) Berova, N.; Nakanishi, K. In *Circular Dichroism*; Berova, N., Nakanishi, K., Woody, R. W., Eds.; Wiley-VCH: New York, 2000.
(7) Balaz, M.; Holmes, A. E.; Benedetti, M.; Rodriguez, P. C.; Berova, N.; Nakanishi, K.; Proni, G. *J. Am. Chem. Soc.* **2005**, *127*, 4172−4173.

Chart 1. Structure of the **Sa** Linker, Capped Hairpins, and Reference Hairpins

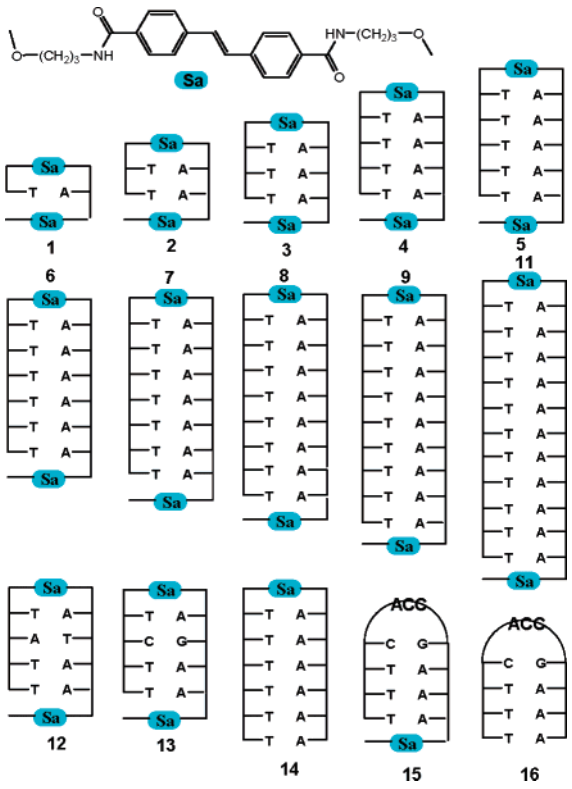

We report here the results of a detailed experimental and molecular dynamics (MD) investigation of the structure, thermodynamics, and absorption and circular dichroism spectroscopy of the complete family of capped hairpin conjugates **1**−**11** and the related hairpin structures **12**−**16** (Chart 1). A single base pair is found to be sufficient to assemble a stable stacked structure with parallel stilbene chromophores. Incremental addition of A:T base pairs results in a nearly constant change in the entropy and enthalpy of base pairing and an increase in the distance and dihedral angle between the long axes of the two stilbenes. Weak exciton coupling between the two stilbenes results in a small shift in the UV absorption maximum for capped hairpin **1** but no observable change for the other conjugates. In contrast, EC-CD can be observed even for conjugate **11**, which has 11 intervening base pairs. Good agreement is observed between experimental spectra and spectra calculated using a structural model based on either an idealized B-DNA geometry or the minimized geometries obtained from MD simulations.

These results also provide important tests for atomistic theoretical models of DNA, such as have been developed for the Amber force field.[8] Past molecular dynamics studies of short double-stranded oligonucleotides[9] have demonstrated the ability of Amber 95[10] to generate stable helical structures that reproduce crystallographic data as well as information about the counterion distributions inferred from other models. With the EC-CD data, it is possible to further test the capabilities of Amber in

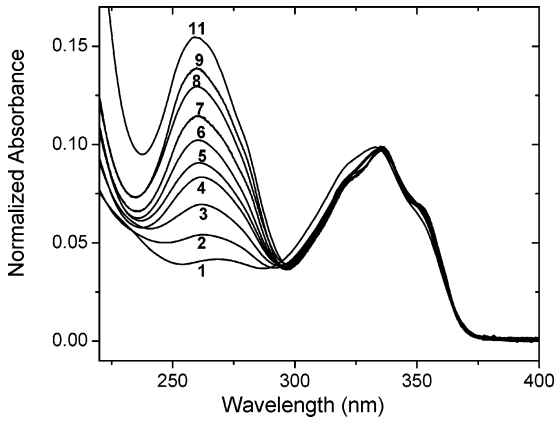

Figure 1. UV absorption spectra of conjugates **1**−**11** in 10 mM sodium phosphate, pH 7.2, containing 0.1 M NaCl (spectra normalized for constant 340 nm absorbance).

describing solution structures with the added complexity of adding hairpin structures (requiring parameters beyond those available in the standard force field) to the DNA description. In addition, these data make it possible to study extremely short duplexes (with as few as one base pair), testing their thermal stability under conditions where normal DNA duplexes are not stable.

Results

UV Spectra and Thermal Dissociation Profiles. The preparation of conjugates **1**−**15** is described in the Experimental Section. The UV absorption spectra of conjugates **1**−**11** are shown in Figure 1. The short-wavelength absorption band near 260 nm occurs in a region where the **Sa** chromophore absorbs weakly and thus is dominated by the absorption of the base pairs. The intensity of this band increases and the band maximum (λ_{max}) shifts to shorter wavelength as the number of A:T base pairs increases, converging on a constant value of 260 nm for six or more base pairs. The long-wavelength band beyond 300 nm is assigned to the lowest energy, allowed $\pi-\pi^*$ transition ($\epsilon = 35\,000$ cm^2 mol^{-1}) of the stilbenedicarboxamide chromophore.[11] The band maximum is at 330 nm for $n = 1$ and at 335 ± 1 nm for the other end-capped hairpins. The ratio of 260 nm/330 nm intensity increases with the length of the base-pair domain.

The temperature dependence of the UV absorbance determined in aqueous buffer containing 0.1 M NaCl is shown in Figure 2a for conjugates **1** and **2** and in Figure 2b for **3**−**9** and **11**. Hyperchromism is observed at 260 nm and hypochromism at 340 nm for all of the conjugates. In all cases, cooling curves display only slight hysteresis when compared to the heating curves shown in Figure 2. Melting temperatures obtained from the first derivatives of these profiles and thermodynamics parameters obtained from curve-fitting are reported in Table 1 for the conjugates **1**−**16**. Similar values of T_M are obtained for both **1** and **2** using the 260 and the 340 nm profiles. Values of T_M increase with the length of the base-pair domain for **1**−**6** but decrease for longer base-pair domains. The melting transitions continue to sharpen as the base-pair domain lengthens.

Circular Dichroism Spectra. The CD spectra of poly(dA):poly(dT) and conjugates **1**−**16** are shown in Figure 3. The

(8) Kollman, P. A. *Chem. Rev.* **1993**, *93*, 2395−2417.
(9) Young, M. A.; Ravishanker, G.; Beveridge, D. L. *Biophys. J.* **1997**, *73*, 2313−2336.
(10) Cornell, W. D.; Cieplak, P.; Bayly, C. I.; Gould, I. R.; Merz, K. M.; Ferguson, D. M.; Spellmeyer, D. C.; Fox, T.; Caldwell, J. W.; Kollman, P. A. *J. Am. Chem. Soc.* **1996**, *118*, 2309−2309.
(11) Lewis, F. D.; Wu, T.; Liu, X.; Letsinger, R. L.; Greenfield, S. R.; Miller, S. E.; Wasielewski, M. R. *J. Am. Chem. Soc.* **2000**, *122*, 2889−2902.

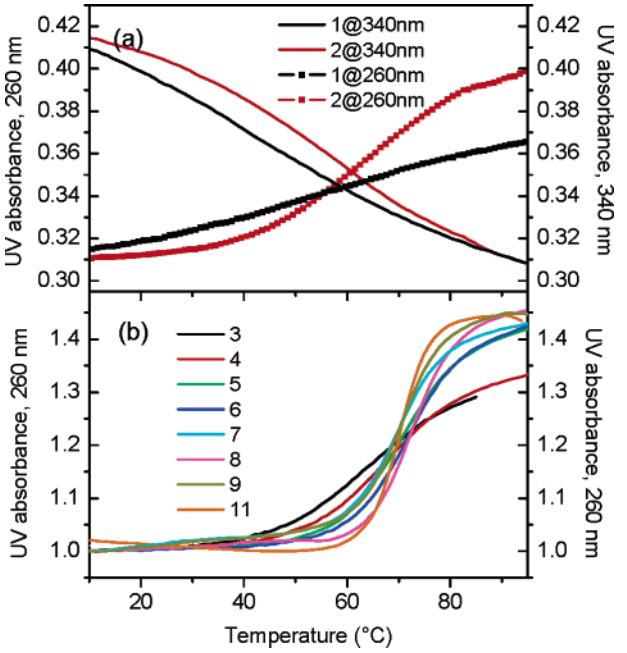

Figure 2. Thermal dissociation profiles for (a) conjugates **1** and **2** determined at 260 and 340 nm and (b) conjugates **3**−**11** determined at 260 nm.

Table 1. Melting Temperatures[a] and Thermodynamic Data[b] for End-Capped Hairpins **Sa**(*n*)**Sa** and Related Hairpins[c]

conjugate	T_M, °C	$-\Delta H°$, kcal/mol	$-\Delta S°$, eu	$-\Delta G°$, kcal/mol
1	48.9 (53.2)[d]			
2	62.6	21.3	63.5	2.4
3	63.8	26.9	80.1	3.0
4	67.6	31.8	92.1	3.9
5	70.1	38.2	111.1	5.0
6	72.1	42.4	122.0	5.8
7	70.0	49.6	144.5	6.5
8	72.5	57.9	167.6	8.0
9	71.0	63.3	183.9	8.5
11	70.6	72.1	209.8	9.5
14	62.1	30.8	91.5	3.5
15	53.4	29.5	90.59	2.49
16	35.6	20.38	66.13	0.66

[a] Melting temperatures obtained from the first derivative of the thermal dissociation profiles in Figure 2. Values of T_M for **12** and **13** are 69.1 and 71.0 °C, respectively. [b] Thermodynamic data obtained from the thermal dissociation profiles by the method of ref 19. [c] See Chart 1 for hairpin and end-capped hairpin structures. [d] Value obtained with 1.0 M NaCl. Thermodynamic data cannot be obtained for **1** due to the breadth of the melting transition.

spectra of hairpins **14** and **15** (Figure 3a) are similar to the spectrum of poly(dA):poly(dT) in the base-pair region (190−290 nm), aside from the more pronounced positive band at 260 nm for poly(dA):poly(dT). The CD spectra of conjugates **1** and **2** do not display well-resolved maxima or minima in the base-pair region; however, conjugates **3**−**11** (Figure 3b) have spectra which resemble those of poly(dA):poly(dT). Additional base pairs lead to sharpening of the maxima and minima and the appearance of a 260 nm shoulder characteristic of poly(dA):poly(dT) (Figure 3a).[12] The CD spectra of conjugates **12** and **13** (Figure 3b) in the base-pair region do not resemble those of **4**.

Weak negative bands are observed for **14** and **15** between 300 and 350 nm. These are assigned to induced CD of the stilbene chromophore. At wavelengths longer than 290 nm, the

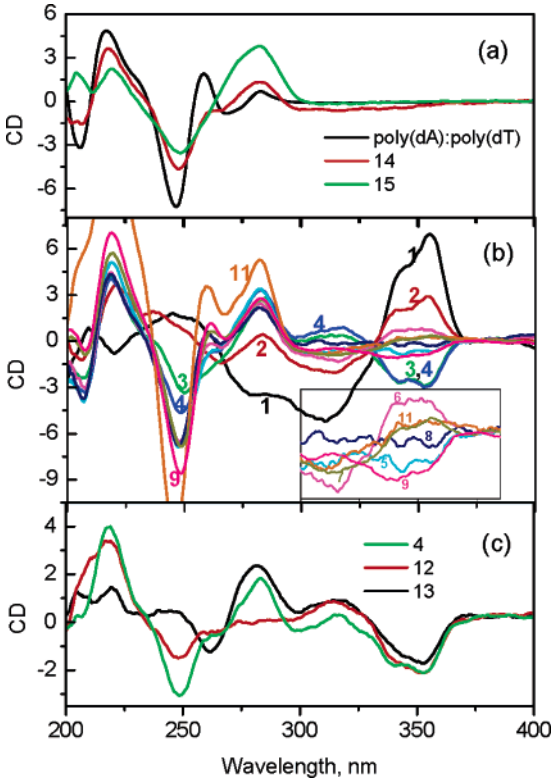

Figure 3. Circular dichroism spectra of (a) poly(dA):poly(dT) and conjugates **14** and **15**, (b) conjugates **1**−**11**, and (c) conjugates **4**, **12**, and **13**.

CD spectra of **1**−**13** are biphasic as a consequence of exciton coupling (EC) between the two stilbene chromophores (see Discussion). Both the sign and the amplitude of the EC-CD spectra depend on the number of base pairs separating the two chromophores. Positive Cotton effects (+/− pattern) are observed for **1**, **2**, **6**, **7**, and **11**, whereas negative Cotton effects (−/+ pattern) are observed for **3**, **4**, **5**, **8**, and **9**. The relative intensities decrease in the order **1** > **2** > **4** ∼ **3** > **6** > **9** > **5** > **7** ∼ **11** > **8**. The EC-CD spectra of **4**, **12**, and **13** are similar at wavelengths longer than 290 nm.

The temperature dependence of the CD spectra has been determined for conjugates **4** (Figure 4) and **6** (provided as Supporting Information, Figure S1). The intensities of both the 247 nm band, assigned to the base-pair domain, and the 347 nm band, assigned to **Sa**−**Sa** exciton coupling, decrease with increasing temperature. Thermal dissociation profiles derived from CD data for both **4** and **6** are provided as Supporting Information (Figures S2 and S3). The half-melting temperatures obtained from the derivative of plots of $\Delta\epsilon$ vs T for **4** are 65 °C at 247 nm and 60 °C at 347 nm. In the case of **6**, the half-melting temperatures are 70 °C at both 247 and 347 nm. These values are slightly lower than the T_M values obtained from the UV melting curves (Table 1).

Molecular Dynamics Simulation. The methods used to construct minimized structures and run MD simulations for the capped hairpins are described in the Experimental Section. Averaged structures obtained from MD simulations for several conjugates are shown in Figure 5. Plots of the MD-simulated geometries (root-mean-square deviation (RMSd), dihedral angle,

(12) Johnson, W. C. In *Landolt−Börnstein, Group VII*; Saenger, W., Ed.; Springer-Verlag: Berlin, 1990; Vol. I, pp 1−24.

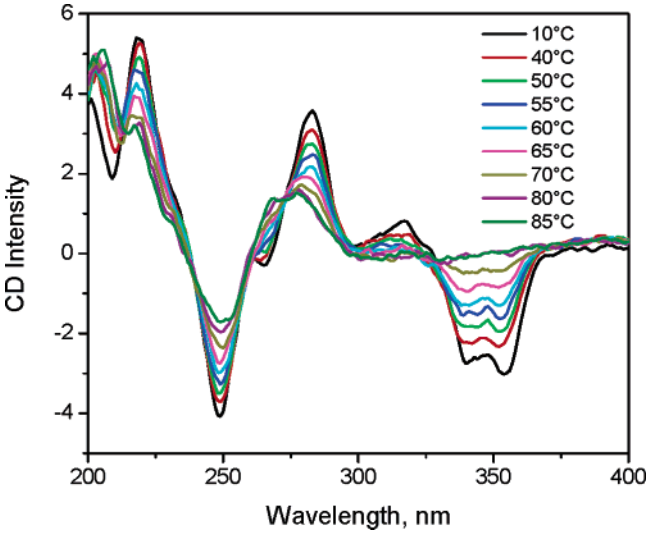

Figure 4. Temperature-dependent CD spectra of conjugate **4** in 0.1 M NaCl, 10 mM phosphate (pH 7.2).

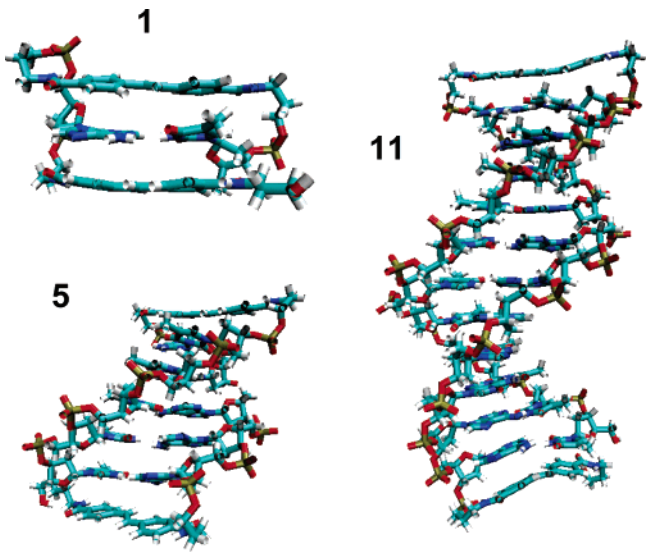

Figure 5. Snapshots of averaged structures obtained from MD simulations for conjugates **1**, **5**, and **11**. Water molecules and counterions were deleted for better viewing.

and distance between stilbenes) for **5** as a function of simulation time are shown in Figure 6. The RMSd's increase with the length of the base-pair domain. The RMSd's for **11** are similar to those for the duplex dA_{11}:dT_{11} (Figure S4). Plots of the averaged dihedral angle and distance between stilbene chromophores vs the number of intervening base pairs are linear with slopes of 34.8 ± 0.8° and 3.36 ± 0.03 Å, in accord with B′-DNA structures (Figure S5). The average angle and distance and calculated fluctuations are reported in Table 2. These values do not display systematic dependence on the length of the duplex base-pair domain.

Attempts to simulate the melting of the capped hairpins were unsuccessful, even in the case of **1** (simulation time = 40 ns at 350 K). Beginning with an unfolded structure for **1**, the formation of a π-stacked structure (Figure 5) occurred within 1 ns at 300 K. A video clip of the folding process is provided as Supporting Information. By way of comparison, a **Sa**-linked hairpin possessing a single base pair required 16 ns to break its A:T hydrogen bond at 300 K.

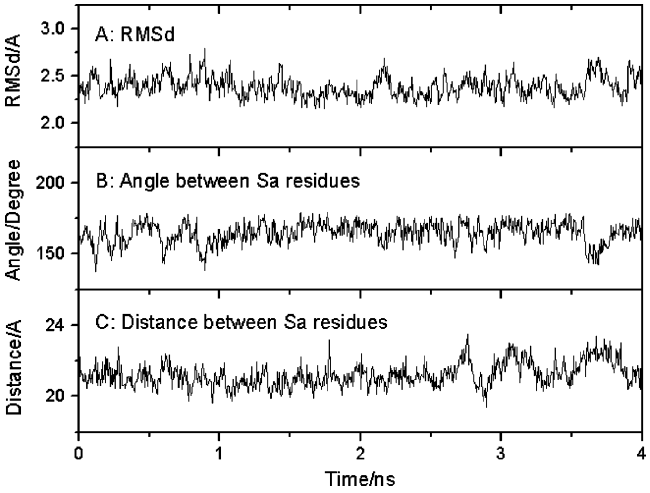

Figure 6. (A) Overall RMS deviation from the MD averaged structure (Å). (B) Fluctuations in the angle between the **Sa** long axes (degrees). (C) Fluctuations in the center-to-center distance between **Sa** chromophores (Å) for conjugate **5**.

Table 2. Average Angle and Distance between Stilbene Long Axes and Their Fluctuation Obtained from MD Simulations

conjugate	angle (degrees)	distance R_{ij} (Å)
1	33 ± 12	7.2 ± 0.3
2	59 ± 13	11.7 ± 0.7
3	102 ± 18	14.3 ± 0.7
4	131 ± 15	17.7 ± 0.6
5	162 ± 8	21.0 ± 0.5
6	213 ± 10	24.2 ± 0.6
8	257 ± 12	30.8 ± 0.6
11	382 ± 9	40.8 ± 0.8

Discussion

Conjugate Structure and Thermodynamic Stability. The synthesis of exceptionally stable synthetic DNA hairpins possessing a **Sa** linker joining a poly(dA):poly(dT) base-pair domain was initially reported by Letsinger and Wu.[13] The crystal structure of a stilbenediether-linked hairpin similar to **14** has been reported by Egli and co-workers and found to have a classic B-DNA base-pair domain with the stilbene π-stacked with the adjacent base pair.[14] The choice of poly(dA):poly(dT) duplex domains, known as A-tracts, was based on their regular structure as well as simplicity of synthesis.[15] A-tracts adopt a structural variant of B-DNA known as B′-DNA, which possesses a strong propeller twist and groove narrowing in the 5′→3′ direction. The helical pitch of B′-DNA is slightly smaller than that for B-DNA (34° vs 36°). A-tracts are reported to be more resistant to base-pair opening than normal B-DNA possessing mixtures of A:T and G:C base pairs.[16]

(13) Letsinger, R. L.; Wu, T. *J. Am. Chem. Soc.* **1995**, *117*, 7323−7328.
(14) (a) Lewis, F. D.; Liu, X.; Wu, Y.; Miller, S. E.; Wasielewski, M. R.; Letsinger, R. L.; Sanishvili, R.; Joachimiak, A.; Tereshko, V.; Egli, M. *J. Am. Chem. Soc.* **1999**, *121*, 9905−9906. (b) Egli, M.; Tereshko, V.; Mushudov, G. N.; Sanishvili, R.; Liu, X.; Lewis, F. D. *J. Am. Chem. Soc.* **2003**, *125*, 10842−10849.
(15) (a) Nelson, H. C. M.; Finch, J. T.; Bonaventura, F. L.; Klug, A. *Nature* **1987**, *330*, 221−226. (b) Dickerson, R. E.; Goodsell, D. S.; Niedel, S. *Proc. Natl. Acad. Sci. U.S.A.* **1994**, *91*, 3579−3583. (c) Woods, K. K.; Maehigashi, T.; Howerton, S. B.; Sines, C. C.; Tannenbaum, S.; Williams, L. D. *J. Am. Chem. Soc.* **2004**, *126*, 15330−15331.
(16) Giudice, E.; Lavery, R. *J. Am. Chem. Soc.* **2003**, *125*, 4998−4999.

Averaged structures for conjugates **1**, **5**, and **11** obtained from molecular dynamics simulations are shown in Figure 5. The average pitch per base pair obtained from MD simulations for conjugates **1**−**11** is 34.8 ± 0.8°, and the average height per base pair is 3.36 ± 0.03 Å. These values are intermediate between those for B-DNA and B′-DNA. The MD-averaged angles of the **Sa** residues with respect to the nearest DNA base pairs were also calculated. The turning angles of both of the **Sa** residues are in the same direction as the right-hand helix of the DNA. The average angle of the hairpin **Sa** residues relative to the adjacent base pair is 34 ± 6°, somewhat larger than the value of 17° obtained from the crystal structure of a stilbene-diether-linked hairpin.[14] The calculated angle for the capping **Sa** residues is 8 ± 4°. With both ends connecting to the DNA, the hairpin **Sa** residue is forced to adopt a larger angle with respect to the nearest DNA base pair in order to fully extend its trimethylene chain. The shorter, more flexible diethylene chain in the stilbenediether hairpin may allow a smaller turning angle. The capping **Sa** residue is much more flexible and is able to adopt a conformation more nearly parallel to the DNA base-pair long axis, thereby maximizing the hydrophobic and stacking interactions. Tuma et al.[17] have recently reported that the long axis of a capping trimethoxystilbene group is aligned nearly parallel to the adjacent base pair in a self-complementary DNA hexamer, based on solution-phase NMR data.

The MD simulations provide information about the time-dependent fluxional nature of the capped hairpins, as shown for conjugate **5** in Figure 6. Fluctuations in the average angle and distance between the stilbenes (Table 2) do not increase appreciably as the base-pair domain becomes longer. This suggests that an increase in twisting angle or base stacking distance in one part of the duplex may be compensated for by a decrease in another part of the duplex. The RMSd fluctuations for the conjugate **11** and the duplex dA_{11}-dT_{11} are similar (Figure S4). Thus, the stilbenes do not constrain the conformational freedom of the base-pair domain. Plausibly, the stilbenes protect the ends of the base-pair domains from end-fraying, a process which is not observed in the MD simulations.

Experimental evidence for the formation of B′-DNA structures by both **Sa**-linked hairpins and capped hairpins is provided by their CD spectra in the 200−290 spectral region (Figure 3), which is dominated by the base-pair signals. The CD spectrum of **11** (Figure 3b) closely resembles that of poly(dA):poly(dT) (Figure 3a).[12] Conjugates with as few as three or four A:T base pairs have CD spectra with maxima and minima similar to those of the longer conjugates. Disruption of the A-tract structure by reversal of a single base pair in **12** or introduction of a G:C base pair in **13** results in gross changes in the CD spectra (Figure 3c). The thermal dissociation profiles shown in Figure 2b display a progressive increase in both the percent hyperchromicity and the sharpness of the melting transition as the number of base pairs in the capped hairpins is increased from 3 to 11. Even in the case of conjugate **1**, a significant increase in the 260 nm absorption and a decrease in the 340 nm absorption are observed upon heating from 0 to 95 °C (Figure 2a). The derivatives of both the 260 and 340 nm thermal dissociation profiles obtained in 0.1 M NaCl solution provide values of $T_M \approx 49$ °C for **1** (Table 1). The formation of a stacked structure around a single base pair in **1** (Figure 5) is supported by MD simulations of the folding of an extended conformation in water, which occurs within 1 ns at room temperature (video clip in the Supporting Information).

Curve-fitting of the 260 nm UV thermal dissociation profiles shown in Figure 2 using the method of Marky and Breslauer[18] provides the thermodynamics parameters for conjugate melting summarized in Table 1. Both the enthalpy and entropy of base pairing ($-\Delta H°$ and $-\Delta S°$) are seen to increase as the number of base pairs increases. Plots of $\Delta H°$ and $\Delta S°$ vs the number of base pairs for conjugates **2**−**6**, **8**, and **11** are linear and provide values of $\Delta\Delta H° = 5.8 \pm 0.9$ kcal/mol and $\Delta\Delta S° = 16.6 \pm 0.3$ eu. These values can be compared to values of $\Delta\Delta H° = 7.9$ kcal/mol and $\Delta\Delta S° = 21.3$ eu per A:T base pair (in 0.1 M NaCl) provided by the model of SantaLucia for duplex melting.[19] The smaller enthalpy and entropy for the conjugates may reflect the influence of the linker and end-cap on the melting process.

Comparison of the T_M values for conjugates **6** vs **14** (Table 1) shows that a 3′-capping stilbene increases the melting temperature by ca. 10 °C. The thermodynamic parameters for conjugates **6** vs **14** indicate that the 3′-capping stilbene chromophore increases the stability of the hairpin by 2.3 kcal/mol. A somewhat smaller value, 1.8 kcal/mol, is obtained by comparison of the capped hairpin **15** with hairpin **16**, both of which have the same ACC loop region and base-pair domain. Increased duplex thermal stability has previously been observed for stilbenes and other aromatic capping groups when attached to self-complementary oligonucleotides.[20,21]

The temperature-dependent CD spectra of conjugates **4** (Figure 4) and **6** (Figure S1) have 247 and 347 nm thermal dissociation profiles (Figures S2 and S3) which are similar to their 260 nm UV profiles (Figure 2b). The 247 and 347 nm CD bands are dominated by exciton coupling within the base pairs and between the stilbenes, respectively. The slightly lower T_M values obtained from the 247 nm CD vs UV profiles may reflect the sparser data set used to obtain the CD profiles. The 347 nm CD T_M value for **6** is similar to its 247 nm value, whereas the 347 nm value for **4** is somewhat lower than its 247 nm value. The similar values at both wavelengths are consistent with a simple two-state model for capped hairpin melting in which unstacking of the stilbene end-cap and dissociation of the A:T base pairs occur cooperatively rather than sequentially. There is no evidence from either the UV or CD spectra for base-pair "premelting" behavior, such as has been reported for poly(dA)-poly(dT).[22] The cooperative melting of the capped hairpins stands in contrast to the non-cooperative melting of the duplex formed between two complementary porphyrin−8-mer conjugates studied by Balaz et al.[7] Half-melting of the porphyrin−porphyrin EC-CD signal occurs at much lower temperatures than half-melting in the base-pair CD spectrum. This most likely reflects poor alignment of the chromophores with the terminal base pairs. In addition, the porphyrin capping groups appear to destabilize rather than stabilize the duplex.

(17) Tuma, J.; Paulini, R.; Rojas Stutz, J. A.; Richert, C. *Biochemistry* **2004**, *43*, 15680−15687.

(18) Marky, L. A.; Breslauer, K. J. *Biopolymers* **1987**, *26*, 1601−1620.
(19) SantaLucia, J., Jr.; Allawi, H. T.; Seneviratne, P. A. *Biochemistry* **1996**, *35*, 3555−3562.
(20) Dogan, Z.; Paulini, R.; Rojas Stutz, J. A.; Narayanan, S.; Richert, C. *J. Am. Chem. Soc.* **2004**, *126*, 4762−4763.
(21) Guckian, K. M.; Schweitzer, B. A.; Ren, R. X. F.; Sheils, C. J.; Tahmassebi, D. C.; Kool, E. T. *J. Am. Chem. Soc.* **2000**, *122*, 2213−2222.
(22) (a) Herrera, J. E.; Chaires, J. B. *Biochemistry* **1989**, *28*, 1993−2000. (b) Mukerji, I.; Williams, A. P. *Biochemistry* **2002**, *41*, 69−77.

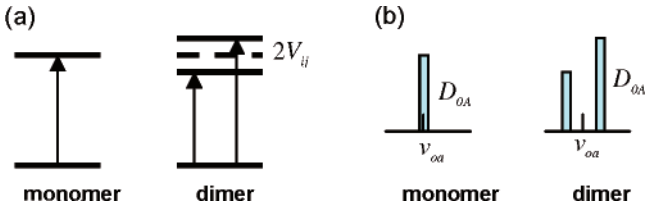

Figure 7. (a) Energy levels for a monomer and dimer, showing the exciton splitting $2V_{ij}$, and (b) spectra of a monomer and dimer, showing band intensities D_{0A} (after ref 23).

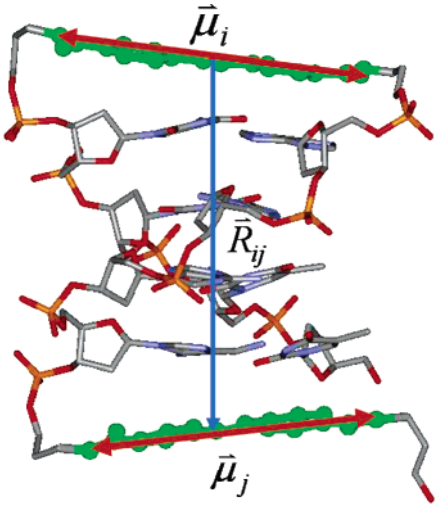

Figure 8. MD-minimized structure of conjugate **4** with superimposed stilbene transition dipoles and distance vector.

Absorption Spectra. The long-wavelength absorption bands of conjugates **1**−**11** (Figure 1) are assigned to the lowest energy, allowed $\pi-\pi^*$ transition of the stilbenedicarboxamide chromophore.[11] The band maximum is at 330 nm for **1** and at 335 ± 1 nm for the other end-capped hairpins. The blue-shift for **1** is attributed to exciton coupling between the two stilbene chromophores. Exciton coupling between two identical chromophores is expected to result in the appearance of both a red-shifted band and a blue-shifted band (Figure 7), with an exciton (Davydov) splitting $2V_{ij}$ determined by eq 1a,[23]

$$V_{ij} \approx (\vec{\mu}_i \cdot \vec{\mu}_j) R_{ij}^{-3} - 3(\vec{\mu}_i \cdot \vec{R}_{ij})(\vec{R}_{ij} \cdot \vec{\mu}_j) R_{ij}^{-5} \quad (1a)$$

$$V_{ij} \approx (\vec{\mu}_i \cdot \vec{\mu}_j) R_{ij}^{-3} \quad (1b)$$

where μ_i and μ_j are the transition dipole moments of the two stilbenes (molar absorbance = 3.5×10^4 and $\mu = 6.7$ D) and R_{ij} is the distance between them. A MD-minimized structure for **4** with superimposed vectors is shown in Figure 8. The stilbene transition dipoles are long-axis polarized[24] and approximately perpendicular to the distance vector, permitting the use of a simplified form of eq 1a provided in eq 1b.

Calculated values of V_{ij} for capped hairpins with 1−16 base-pair domains are shown in Figure 9a and are seen to decrease from 560 cm^{-1} for **1** to 65 cm^{-1} for **2**.[25] The relative intensity

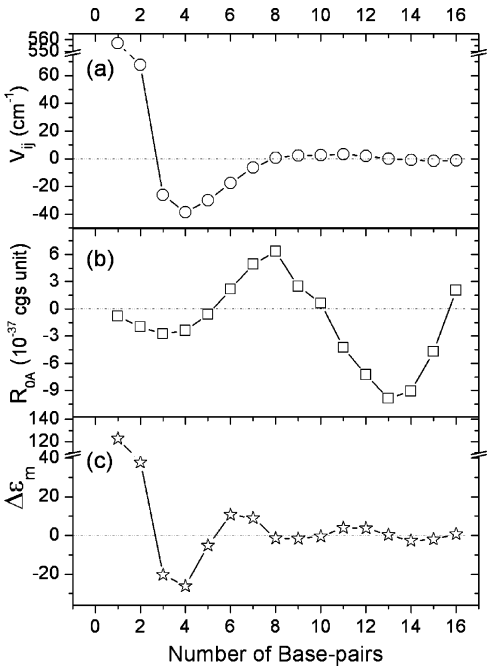

Figure 9. Calculated values of (a) V_{ij} (eq 1a), (b) R_{0A} (eq 3), and (c) the magnitude and sign of the EC-CD spectrum of the **Sa**(*n*)**Sa** end-capped hairpins vs the number of intervening A:T base pairs obtained assuming idealized B-DNA geometries.

of the two exciton-coupled absorption bands (Figure 7b) is determined by the angle between the dipole moments. For an angle near 0°, most of the intensity is in the blue-shifted band. The calculated absorption shift for **1** is 5.4 nm, in good agreement with the observed shift (Figure 1). The absence of absorption spectral shifts for end-capped hairpins with ≥2 base pairs is consistent with their much smaller calculated values of V_{ij} (Figure 9a).

Exciton-Coupled Circular Dichroism. The CD spectra of conjugates **14** and **15** (Figure 3a) display weak, structureless negative bands in the region of the stilbene absorption (300−350 nm). These bands are assigned to the induced CD of the **Sa** chromophore. The appearance of these bands is similar to the appearance of those of achiral intercalators in which the long axis of the intercalator is approximately parallel to the long axis of the adjacent base pair.[26] The CD spectra of **1**−**11** (Figure 3b) are more complex, displaying two bands at long wavelengths with either a +/− or a −/+ pattern. These CD bands are attributed to exciton coupling between the **Sa** chromophores.[6]

Exciton coupling between two identical chromophores results in CD spectra for the individual chromophores having opposite signs and equal intensity (Figure 10). Even very weak coupling can result in a bisignate spectrum (Cotton effect). The rotational strength, R_{0A}, of an isolated CD transition is determined by the imaginary part of the dot product between the electronic and magnetic transition dipoles (eq 2).[23,27] For two interacting chromophores, the rotational strength for each of the split CD bands is dominated by the coupled oscillator or exciton term, which can be defined in simplified form by eq 3,

$$R_{0A} = imag\{\langle\Psi_0|\hat{\vec{\mu}}|\Psi_A\rangle \cdot \langle\Psi_A|\hat{\vec{m}}|\Psi_0\rangle\} \quad (2)$$

$$R_{0A\pm} \approx \pm \frac{\pi}{2\lambda} \vec{R}_{ij} \cdot \vec{\mu}_j \times \vec{\mu}_i \quad (3)$$

where R_{ij} is the vector between the centers of the two monomers

(23) Cantor, C. R.; Schimmel, P. R. *Biophysical Chemistry*; W. H. Freeman: New York, 1980; Vol. 2.
(24) Champagne, B. B.; Pfanstiel, J. F.; Plusquellic, D. F.; Pratt, D. W.; Van Herpen, W. M.; Meerts, W. L. *J. Phys. Chem.* **1990**, *94*, 6−8.
(25) Idealized B-DNA geometries with turning angles of 17° for both chromophores, rather than MD-minimized geometries, have been used in these calculations. The angles between chromophores obtained from MD simulations are larger by 8° than those used in these calculations.

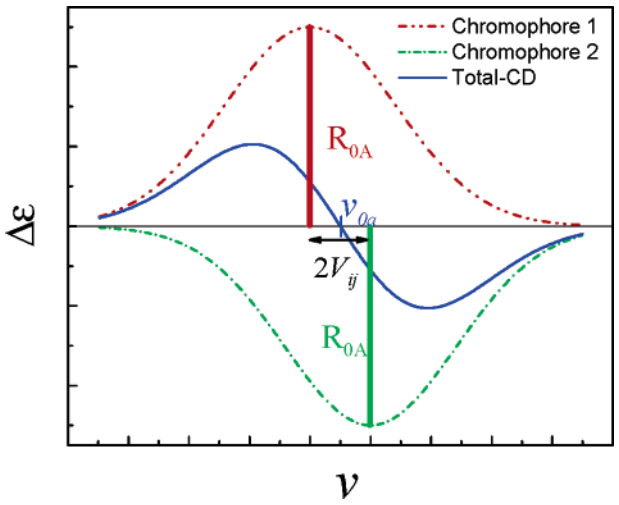

Figure 10. CD spectra of a dimer with identical chromophores. Dashed lines show the contributions to the spectra from the two exciton split bands and the solid line shows the expected observed spectrum (after ref 23).

and μ_i and μ_j are their electronic transition dipole moments. The calculated values of $R_{0A\pm}$ shown in Figure 9b display an $R_{ij} \sin \theta$ dependence, where θ is the angle between the two stilbene transition dipoles.[25] However, since the splitting depends on R_{ij}^{-3} (eq 1b), when the Davydov splitting $2V_{ij}$ is small, the CD intensity ($\Delta\epsilon$, eq 4a) decreases approximately as $R_{ij}^{-2} \sin(2\theta)$, as shown in Figure 9c.[27]

$$\Delta\epsilon \approx \pm \frac{\pi}{2\lambda} \vec{R}_{ij} \cdot \vec{\mu}_i \times \vec{\mu}_j \cdot V_{ij} \qquad (4a)$$

$$\Delta\epsilon \approx \pm \frac{\pi}{4\lambda} \mu_i^2 \mu_j^2 R_{ij}^{-2} \sin(2\theta) \qquad (4b)$$

Since the distance vector is perpendicular to the stilbene transition dipole vectors (Figure 8), eq 4a can be simplified to provide eq 4b.[5] Increasing the number of base pairs separating the chromophores changes both the sign and intensity of the CD spectrum as a consequence of the changes in the distance and dihedral angle between the chromophores. According to eq 4b, the CD intensity should display an R_{ij}^{-2} dependence and have maximum intensity when the dihedral angle θ between the chromophore transition dipoles is 45° or 135° (with an inversion in sign) but zero intensity when the chromophore transition dipoles are parallel or perpendicular.

A plot of $\Delta\epsilon$ vs $R_{ij}^{-2} \sin(2\theta)$ obtained using the experimental CD data (Figure 3b) and calculated geometries for conjugates **1**−**11** is shown in Figure 11. A linear fit of the data for **2**−**11** has a correlation coefficient of 0.98 and a standard deviation of 0.44. The deviation from the linear fit for conjugate **1** is an expected consequence of its much larger value of V_{ij} (Figure 9a) and our neglect of the second term in eq 1a, which will be most important in the case of **1**. Also, since the calculated value of θ for **1** is 33°, a smaller angle would move the calculated value of $R_{ij}^{-2} \sin(2\theta)$ toward the linear fit in Figure 11.

The linear correlation shown in Figure 11 requires that the geometric model assumed for the capped hairpins is valid, even

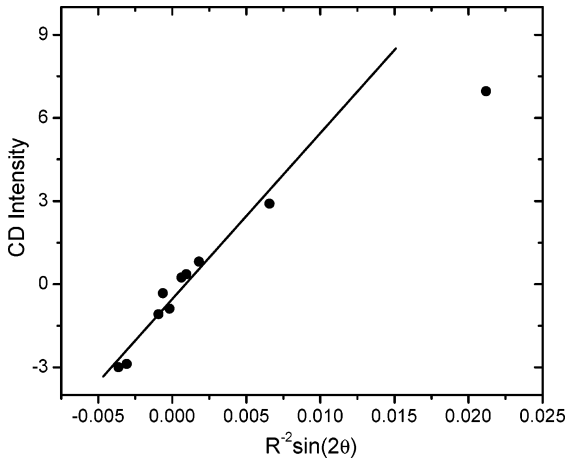

Figure 11. Intensity of the 340 nm CD band vs $R_{ij}^{-2} \sin(2\theta)$ for conjugates **1**−**11**. The line is the least-squares fit to the data omitting the data point for **1**.

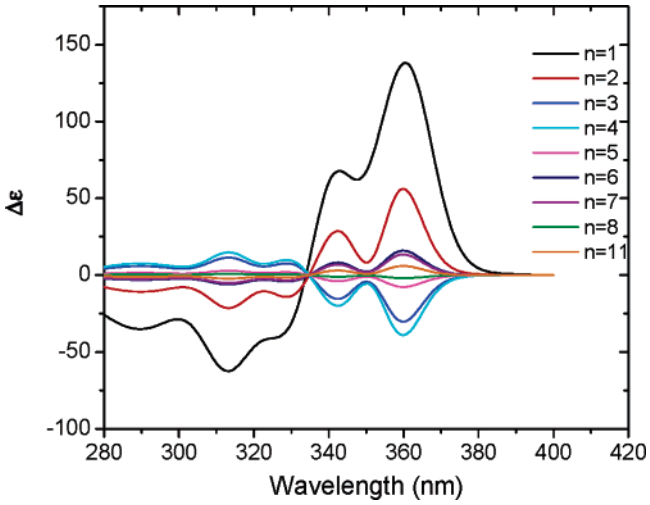

Figure 12. Simulated CD spectra for conjugates **1**−**8** and **11** obtained following the method of Harada and Nakanishi[27] using four Gaussians to simulate the **Sa** absorption spectrum.

for the shortest base-pair domains. An error in the estimated **Sa**−**Sa** vector by as little as ±20° would be reflected in an inversion in the sign of the Cotton effect at a larger or smaller value of *N*. Thus, one or two base pairs are sufficient to establish the geometry of conjugates with longer A-tracts.

It is interesting to note that the EC-CD spectra of conjugates **12** and **13** are similar to the spectrum of **4** even though their base-pair CD regions are markedly different (Figure 3c). This requires that the three conjugates have similar structures and suggests that the use of DNA as a helical scaffold is not limited to A-tract base-pair domains.

Simulated EC-CD Spectra. Simulated EC-CD spectra, obtained by the method of Harada and Nakanishi[27] using B-DNA structural parameters as described in the Supporting Information, are shown in Figure 12. The calculated EC-CD spectra reproduce the gross features of the observed spectra, including inversions in the sign and intensity of the spectra with increasing numbers of A:T base pairs and the higher intensity of the longer wavelength bands. The asymmetry (more intense long-wavelength CD band) and vibronic structure observed in the CD spectrum of **1** can be reproduced with remarkable fidelity by modeling the stilbene long-wavelength absorption band as

(26) Ardhammar, M.; Nordén, B.; Kurucsev In *Circular Dichroism, Principles and Applications*; Berova, N., Nakanishi, K., Woody, R. W., Eds.; Wiley-VCH: New York, 2000; pp 741−768.
(27) Harada, N.; Nakanishi, K. *Circular dichroic spectroscopy: exciton coupling in organic stereochemistry*; University Science Books: Mill Valley, CA, 1983.

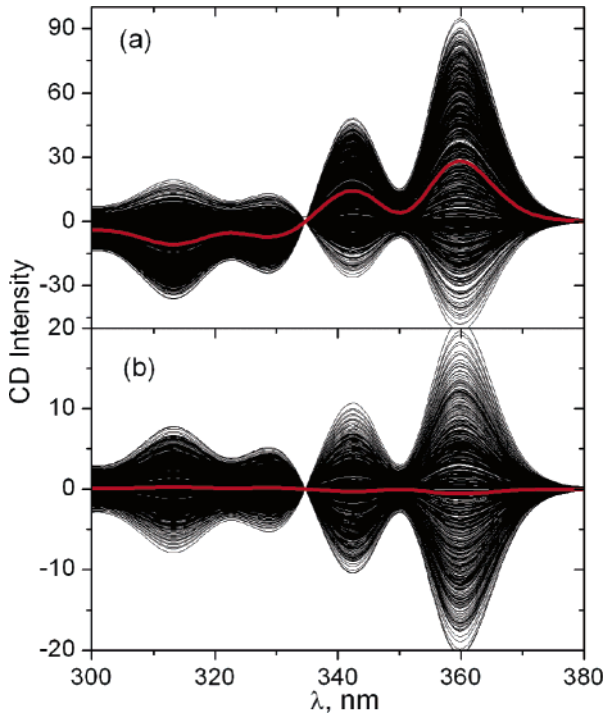

Figure 13. CD spectra for conjugates **2** (a) and **5** (b) calculated from snapshots of MD-simulated geometries and the average CD (red line) obtained from 1194 conformations.

a sum of four Gaussians. However, the calculated spectra overestimate the vibronic structure for the longer capped hairpins. This result might reflect errors in our structural models or interactions of the stilbene chromophores with the solvent and duplex base pairs, both of which are ignored in these calculations.

The effects of conjugate structural fluctuations upon CD spectra can be probed by using the multiple snapshot geometries obtained from MD simulations (Figures 5 and 6) to calculate the EC-CD spectra. Values of V_{ij} (eq 1b) and R_{0A} (eq 3) for different simulated geometries can be used to calculate the EC-CD spectra for these geometries, as shown for conjugates **2** and **5** in Figure 13. Superimposed on the individual calculated spectra is the time-averaged spectrum, which is in reasonable agreement with the sign and relative magnitude of the experimental spectra (Figure 3b). The simulated spectra show that excursions from the average geometry result in changes in EC-CD sign as well as magnitude, but neither broaden the calculated spectra nor predict the relative intensities for several of the conjugates. The absence of broadening is a consequence of the very small exciton coupling V_{ij} between stilbenes. The EC-CD spectra may be more sensitive to thermal fluctuations and geometry changes for some conjugates than for others.

It is, of course, possible that not all of the geometries obtained from Amber simulations correspond to actual solution geometries of the conjugates. As some of us recently observed, comparison of the X-ray scattering patterns for the duplex A_{10}:T_{10} with Amber MD simulations showed that only about 10−30% MD conformers possess geometries consistent with the X-ray scattering experiment.[28] We were also concerned that the capping stilbene might not remain aligned and π-stacked with the adjacent base pair. However, we have recently prepared dumbbell structures in which both stilbenes are covalently linked to both duplex strands and find that both their CD spectra and MD-simulated structures are similar to those of the capped hairpins.[29]

Concluding Remarks. The results described herein provide the initial use of DNA as a helical ruler to investigate both the distance and angular dependence of the interactions between chromophores separated by a base-pair domain. EC-CD is a highly sensitive probe of the helical structure of DNA because of both its pronounced sensitivity to changes in the interchromophore dihedral angle (sin 2θ) and the R^{-2} distance dependence, which results in a more gradual decrease in signal intensity with distance than observed for other long-distance electronic interactions such as fluorescence energy transfer (R^{-6} dependence) or electron tunneling (e^{-R} dependence). Our results demonstrate that atomistic molecular models of the capped hairpin structures provide an excellent description of the EC-CD data, and further reveal the importance of fluctuations in the helical twist angle as a target for future studies.

Whereas this study has focused on the use of DNA as a helical scaffold, the methodology reported here is expected to have applications to the study of small molecule and protein binding to well-defined base-pair domains. For example, binding of an intercalator is expected to increase the distance between capping chromophores but to decrease the angle between their long axes, as a consequence of duplex unwinding.[1] Stilbenedicarboxamide may not be the optimal chromophore for such studies due to its photochemical reactivity and the moderate intensity of its broad 335 nm absorption band (Figure 1). Chromophores such as perylenes[30] and porphyrins[7] have sharper and more intense long-wavelength absorption bands than do the stilbenes, and they have found applications in the study of electronic interactions in oligonucleotide conjugates.

Control of the dihedral angle between chromophore electronic transition dipoles is, however, even more important than chromophore oscillator strength. Stilbenedicarboxamide, both as a hairpin linker and as a capping group, has the advantage of conformational alignment of the electronic transition dipole with the adjacent base pair. The combination of chromophore alignment and sharp, intense absorption bands should permit the observation of EC-CD between chromophores separated by more than 11 base pairs.

In closing, we note that the UV (Figure 1) and CD spectra (Figure 3b) of the capped hairpins in the 190−290 nm (UV−C) spectral region are also dependent on the number of base pairs. Since the stilbene chromophores absorb weakly in this spectral region, these changes reflect electronic interactions between base pairs. The changes in absorption maximum and CD resolution are most evident for conjugates **1**−**5**, suggesting that the electronic interactions responsible for these changes have a persistence length of 4 or 5 base pairs. Analysis of this spectral data is continuing and will be published elsewhere. We are also currently investigating the use of DNA as a helical scaffold in studies of the efficiency of electron- and energy-transfer processes involving donor and acceptor chromophores separated by A-tracts or variable length.[31]

Experimental Section

Materials. The preparation of *trans-N,N′*-bis(3-hydroxylpropyl)-stilbene-4,4′-dicarboxamide (**Sa**) and conversion to its mono-protected,

(28) Zuo, X.; Tiede, D. M. *J. Am. Chem. Soc.* **2005**, *127*, 16−17.

(29) Zhang, L.; Long, H., unpublished results.

mono-activated diol by sequential reaction with 4,4′-dimethoxytrityl chloride and with 2-cyanoethyl diisopropylchlorophosphoramidite have been described.[13,32] Oligonucleotide−stilbenedicarboxamide conjugates were prepared by means of conventional phosphoramidite chemistry using a Millipore Expedite DNA synthesizer following the procedure of Letsinger and Wu.[13] Capped hairpins with **Sa** at the 3′ end were synthesized using a universal solid support. All of the 2′-deoxynucleotide phosphoramidites, DNA synthesizing reagents, and controlled pore glass solid supports (CPG) were purchased from Glen Research (Sterling, VA). Following synthesis, the conjugates were first isolated as trityl-on derivatives by reverse-phase (RP) HPLC, then detritylated in 80% acetic acid for 30 min, and repurified by RP-HPLC as needed. RP-HPLC analysis was carried out on a Dionex chromatograph with a Hewlett-Packard Hypersil ODS-5 column (4.6 × 200 mm) and a 1% gradient of acetonitrile in 0.03 M triethylammonium acetate buffer (pH 7.0) with a flow rate of 1.0 mL/min.

Molecular weights of representative conjugates were determined by means of electrospray ionization mass spectroscopy with a Micromass Quattro II atmospheric pressure ionization (API) spectrometer. Purified oligonucleotide conjugates were further purified by usign a Nensorb 20 nucleic acid purification cartridge (New Life Science Products, Boston, MA) prior to direct loop injection.

Electronic Spectroscopy. UV spectra and thermal dissociation profiles were determined using a Perkin-Elmer Lambda 2 UV spectrophotometer equipped with a Peltier sample holder and a temperature programmer for automatically increasing the temperature at the rate of 0.5 °C/min. Circular dichroism spectra were obtained using a JASCO J-715 spectropolarimeter equipped with a Peltier sample holder and temperature controller. Temperatures were increased at a rate of 0.5 °C/min. Unless otherwise noted, all the spectroscopic studies were done in 0.1 M NaCl, 10 mM phosphate buffer (pH 7.2) using freshly prepared sample solution. EC-CD spectra were studied by using oligonucleotide conjugates with a **Sa** concentration of 4 μM.

Computational Methods. The base-pair domains of the capped hairpin structures were calculated using the AMBER force field[10] by adopting the canonical B-form DNA structure.[33] The charge parameters for the **Sa** linker were obtained using the RESP charge-fitting method[34] by fitting the electrostatic potential of the fully geometry-optimized structure calculated by GAMESS at the RHF/6-31G* level.[35] The **Sa** transition moment obtained from TD-DFT calculations is long-axis polarized, in agreement with experimental data.[24] Capped hairpin structures were obtained by replacing the external base pairs of an (*n* + 2)-mer with **Sa** residues. These structures were then minimized in a vacuum to remove any unfavorable interactions caused by imposing the **Sa** residues. To maintain the B-DNA structure, a force constant of 25.0 kcal/mol·Å was applied on the DNA residues. The minimized structures were then solvated in a TIP3P water box, and sufficient Na^+ ions were added to neutralize the charge on the DNA hairpins.

The AMBER 7.0 program suite[36] was used to run MD simulations with a time step length of 2 fs for conjugates **1**−**6**, **8**, and **11**. Ewald summation was used to handle the long-range forces. Each simulation began with an energy minimization with 25.0 kcal/mol·Å restraints on the **Sa** DNA hairpins, followed by a 50.0 ps MD simulation with the same restraints to heat the systems to 300 K. The system was then minimized again while the restraints were gradually reduced to zero. Finally, the unrestrained system was heated to 300 K and equilibrated at 300 K for 1.0 ns. Conformations of the conjugates were then sampled out every 5.0 ps for another 3.0 ns. The average structures of these 3 ns simulations were compared with the trajectories of the 1.0 ns equilibration simulations by monitoring the root-mean-square deviation (RMSd) to make sure that the structures had reached equilibrium after the initial 1.0 ns simulation runs. Methods used to obtain simulated EC-CD spectra are reported as Supporting Information.

Acknowledgment. This research was supported by grants from the Office of Basic Energy Sciences, U.S. Department of Energy, under contracts DE FG02-96ER14604 (F.D.L.) and W-31-109-ENG-38 (D.M.T.), by DARPA (DURINT program) grant no. F49620-011-0401, and by the Nanoscale Science and Engineering Initiative of the National Science Foundation under NSF Award No. EEC-0118025 (G.C.S.). We thank Julianne M. Kuck for help with the MD simulations.

Supporting Information Available: Temperature-dependent CD spectra for conjugate **6** and CD thermal dissociation profiles for conjugates **4** and **6**, plots of average angle and distance between stilbene chromophores obtained from MD simulations, methods used to obtain simulated CD spectra, and video clip of folding for conjugate **1**. This material is available free of charge via the Internet at http://pubs.acs.org.

JA0539387

(30) Wang, W.; Zhou, H.; Niu, S.; Li, A. D. Q. *J. Am. Chem. Soc.* **2003**, *125*, 5248−5249.
(31) Lewis, F. D.; Zhang, L.; Zuo, X. *J. Am. Chem. Soc.* **2005**, *127*, 10002−10003.
(32) Lewis, F. D.; Wu, Y.; Liu, X. *J. Am. Chem. Soc.* **2002**, *124*, 12165−12173.
(33) Arnott, S.; Campbell-Smith, P. J.; Chandrasekaran, R. In *Handbook of Biochemistry and Molecular Biology*, 3rd ed.; CRC Press: Cleveland, OH, 1976; pp 411−422.
(34) Cieplak, P.; Cornell, W. D.; Bayly, C.; Kollman, P. A. *J. Comput. Chem.* **1995**, *16*, 1357−1377.
(35) Schmidt, M. W.; Baldridge, K. K.; Boatz, J. A.; Elbert, S. T.; Gordon, M. S.; Jensen, J. H.; Koseki, S.; Matsunaga, N.; Nguyen, K. A.; Su, S. J.; Windus, T. L.; Dupuis, M.; Montgomery, J. A. *J. Comput. Chem.* **1993**, *14*, 1347−1363.
(36) *AMBER 7*; University of California, San Francisco, 2002.